Journal of Orthopaedic Surgery and Research

RESEARCH

Open Access

# Effect of collagen-based scaffolds with hydroxyapatite on the repair of cartilage defects in the rabbit knee joint

Xiaoliang He[1], Qiuping Han[1], Yuxin Zhang[1], Huan Zhang[1], Jun Liu[2] and Xiaohui Zhou[1*]

## Abstract

**Background** The repair of articular cartilage defects is always a significant clinical challenge in joint treatment. Therefore, the aim of this study was to investigate that the ColII-HA-CS-HAP scaffolds with BMSCs could repair cartilage defects of knee.

**Methods** Bone marrow mesenchymal stem cells (BMSCs) were extracted from rabbits, identified using immunofluorescence staining, and successfully induced into chondrocytes. Type II collagen (ColII) was isolated from bovine cartilage and constructed into scaffolds with hyaluronic acid, chondroitin sulfate, and hydroxyapatite. Then BMSCs were seeded on the ColII-HA-CS-HAP scaffold to detect biocompatibility.

**Results** The results of DAPI fluorescence staining showed that the number of BMSCs on the ColII-HA-CS-HAP scaffolds increased rapidly after culturing for 12 d. The rabbit knee cartilage defect model with a diameter of approximately 3 mm and a thickness of approximately 4 mm was selected to evaluate the regenerative potential of the scaffolds using histological and immunohistochemical analyses. At 6 months, the regenerated cartilage in the ColII-HA-CS-HAP scaffolds with BMSCs was more similar to that of native cartilage than the ColII-HA-CS-HAP scaffold group.

**Conclusions** Our study proved that the ColII-HA-CS-HAP scaffolds with differentiated BMSCs can produce an excellent healing response and repair cartilage defects successfully in a rabbit model.

**Keywords** BMSCs, Type II collagen (ColII), Cartilage scaffold, Cartilage defect

## Introduction

A variety of three-dimensional (3D) osteochondral scaffolds designed by heterogeneous materials, providing an optimal environment, have the possibility to be used for repairs of knee cartilage [1]. Articular cartilage (AC) is basically composed of water, type II collagen, proteoglycans (PGs) / glycosaminoglycans (including hyaluronic acid, heparin, and chondroitin sulfate) and chondrocytes [2, 3]. Mutations in the COL2A1 gene, encoding type II collagen, can cause a spectrum of rare autosomal-dominant conditions characterized by skeletal dysplasia, short stature, and sensorial defects [4]. Chondroitin sulfate

*Correspondence:
Xiaohui Zhou
zhouxh2003@aliyun.com
[1]College of Food Science and Biology, Hebei University of Science and Technology, NO. 26 Yuxiang Street, Shijiazhang, Hebei 050018, China
[2]College of Food and Biotechnology, Qiqihar University, Qiqihaer, Heilongjiang, China

(CS) is a linear glycan chain mainly composed of repeating disaccharide units of glucuronic acid (GlcA) and *N*-acetylgalactosamine (GalNAc), attaching to specific scaffolds as glycosaminoglycans [5]. CS can assemble multimeric signaling complexes, modulate neurotrophin signaling pathways [6], reduce joint pain and slow structural disease progression [7]. Hyaluronic acid (HA) is a natural polyanionic polymer composed of glucuronic acid and N-acetylglucosamine repeats by a β-1, 4 linkage [8] and is used in tissue regeneration [9]. Hydroxyapatite (HAP) is a natural biocompatible bioceramic compound, that is widely utilized in medicine delivery, tissue engineering and orthopedics [10]. Chondrocytes are the only cells residing in cartilage tissue that maintain the function of cartilage tissue [11]. Autologous chondrocyte transplantation, tissue engineering and cell-based approaches have shown significant improvement in knee function and potential for treating prominent osteopathic cartilage defects [11, 12].

Bone marrow mesenchymal stem cells (BMSCs), which are multipotent stem cells from bone marrow, can be readily obtained and induced to differentiate into cartilage after culture [13]. In vitro, cartilage regeneration from BMSCs is a promising method for functional reconstruction of osteochondral defects and promoting the clinical application of cartilage regeneration technology [14]. Osteoarthritis characterized by pain and disability is the most common, chronic and degenerative joint disorder, and is associated with the aging population and obesity [15]. Maintenance therapy with chondroitin sulfate and hyaluronic acid as a next step providing sustained clinical benefit is recommended in the treatment of knee osteoarthritis [16, 17]. Repairing articular cartilage is an enormous challenge in biomedical engineering because of the poor regenerative capacity of cartilage [18, 19], while cartilage tissue engineering needs supports to overcome degenerative diseases [20, 21].

In this study, to mimic the composition and structure of bone, and inspired by the biomineralization process, we have obtained the tissue engineering cartilage scaffolds (ColII-HA-CS-HAP-BMSCs), which are low-cost, simple operation, green and environmental protection. Finally, we demonstrated scaffolds' efficacy in repairing cartilage using a rabbit model.

## Methods

### Isolation and characterization of BMSCs from New Zealand white rabbit

BMSCs were isolated from 6-month-old New Zealand white (NZW) rabbit (providing and obtaining approval from the animal experiment center of Hebei Medical University, Shijiazhuang, China). All methods were carried out in accordance with relevant guidelines and regulations. All methods are reported in accordance with ARRIVE guidelines (https://arriveguidelines.org). The rabbits were anesthetized by administration of 5% pentobarbital sodium in the ear vein (0.5 mL/kg). Bone marrow cells were obtained by flushing the cavity of the femurs and tibias harvested under sterile conditions, centrifuged at 1000 rpm for 10 min, the supernatants were discarded, and the cells were cultured in low-glucose Dulbecco's modified Eagle's medium (DMEM) supplemented with 10% fetal bovine serum (FBS) and 1% penicillin-streptomycin (Gibco, USA) at 37 °C, in a 5% $CO_2$ cell culture incubator [22]. The medium was replaced every 2 d. When the cells reached 90% confluence, the adherent cells were trypsinized with 3 mL of 0.25% pancreatin (Gibco, USA) for 2 min, harvested and expanded in T-25 flasks (Thermo Fisher Scientific, China).

Toluidine Blue Metachromatic Staining and Immunohistochemical Detection of ColII BMSCs that had undergone three passages were trypsinized with 0.25% pancreatin and cultured on a cell climbing piece for 14 days in DMEM supplemented with 10% FBS, 100 nM dexamethasone, 50 μg/mL L-ascorbic acid 2-phosphate, 40 μg/mL L-proline, 1 mM sodium pyruvate, 1% ITS+, and 10 ng/mL TGFβ3 (Thermo Fisher Scientific, China) [23]. BMSCs were fixed with 4% paraformaldehyde (Wuhan Servicebio Technology Co., Ltd, China) for 30 min, washed with PBS three times, stained with toluidine blue, and treated with 50% glycerol solution (PBS). The cells were examined under a microscope (Primo Star, Carl Zeiss Microscopy Deutschland GmbH, Germany). The cell climbing piece of BMSCs cultured for 14 days was washed with PBS three times, and an added endogenous peroxidase blocker (Shanghai Wellbio Biotechnology Co., Ltd. China) and incubated for 10 min, blocked with 5% BSA for 1 h, incubated with primary antibodies against goat anti-type II collagen (Beijing Biosynthesis Biotechnology Co., Ltd, China) overnight at 4 °C, washed three times with PBS for 3 min, incubated with Goat Anti-Rabbit IgG Fc-HRP (SouthernBiotech, USA) for 20 min, washed three times by PBS for 3 min, incubated with enhanced diaminobenzidine (DAB) chromogenic reagent for 10 min, stained with hematoxylin, rehydrated through a graded series of ethanol washes, deparaffinized in xylene, and examined using Nikon Inverted Routine Microscope Eclipse Ts2 (Nikon Imaging Sales Co., Ltd., China).

After extensive washing with PBS solution, the BMSCs were incubated with secondary antibodies containing fluorescein isothiocyanate (FITC, Beijing Biosynthesis Biotechnology Co., Ltd, China) at 37 °C for 2 h and analyzed by Attune NxT flow cytometry (Thermo Fisher Scientific Co., Ltd, China). The proliferation of BMSCs was evaluated by MTT [3-(4, 5-dimethylthiazol-2-yl)-2, 5-diphenyltetrazolium bromide] assays (Wuhan Servicebio Technology Co., Ltd, China).

### Preparation and characterization of the cross-linking scaffold

The purified collagen (ColII, 0.1 g) extracted from bovine cartilage as previously described [24, 25], hyaluronic acid (HA, 0.01 g), chondroitin sulfate (CS, 0.01 g) and hydroxyapatite (HAP, 0.006 g) were dissolved in 8 mL ultrapure water in turn, stirred by magnetic stirrer (Ronghua, Jintan, China) at 4 ℃, 120 r/min for 6 h. The 50 μL 1-ethyl-3-(3-dimethylaminopropyl)- carbodiimide /N- hydroxysuccinimide (EDC/NHS) cross-linking mixtures (0.05 g/mL EDC and 0.005 g/mL NHS at a ratio of volume 160:1) were added to the ColII-HA-CS-HAP solutions stirring at 4 ℃, 120 r/min for 10 min. Then, the solutions was subpacked into 24 well plates (150 uL/well) and cross-linked at 4 ℃ for 12 h. After cross-linking, the solutions was placed at 4 ℃ for 1 h and −20 ℃ for 4 h, lyophilized at -106 ℃ and 4 KPa by ScanSpeed MaxiVac (Labogene, The Kingdom of Denmark), washed by 0.1 mol/L $Na_2HPO_4$ for 1.5 h with a change of solution every 30 min, poured in 2 mol/L NaCl for 1 h with a change of solution every 20 min, washed with ultrapure water for 30 min, three times. The ColII-CS-HA-HAP cross-linking scaffolds were obtained by lyophilization after 4 h. The biocompatibility, nontoxicity, and biodegradability of ColII-CS-HA-HAP scaffolds were detected by hematoxylin-eosin staining [26] and sectioning technology using mice (provided and obtained approval from the animal experiment center of Hebei Medical University, Shijiazhuang, China).

### DAPI fluorescent stains

Three passages of BMSCs were seeded and cultured in a 37°C, 5% $CO_2$ incubator for 24 h at a concentration of 500 μl/well ($2.5\times10^4$ cells) in 24 well plates, with the ColII-HA-CS-HAP scaffolds sterilized by ethylene oxide. Then the BMSCs were fixed with 4% paraformaldehyde for 15 min, washed with PBS three times, stained with 4′, 6-diamidino-2-phenylindole (DAPI, Beijing Biosynthesis Biotechnology Co., Ltd, China) for 10 min in the dark, washed with PBS three times, added to 50% glycerol solution, and observed using Nikon inverted routine microscope Eclipse Ts2. The morphology and adhesion of BMSCs on the scaffolds were photographed by SEM.

### Rabbit osteoarthritis (OA) model

Twenty-seven NZW rabbits (6 months old) were randomly allocated into three groups: cartilage defect model without treatment group (blank group, $n=9$), ColII-HA-CS-HAP scaffolds sterilized by ethylene oxide (control group, $n=9$), and ColII-HA-CS-HAP scaffolds sterilized by ethylene oxide with BMSCs cultured for 7 d (experimental group, $n=9$). Following anesthesia, the lower limbs of rabbits were shaved and trimmed with iodine volts before surgery. A medial parapatellar incision, including the skin and subcutaneous tissue, was made to expose the femoral trochlea in the knee. The osteochondral injury, which was 3 mm in diameter and 4 mm in depth, was caused by an orthopedic drill with a perforated core in the middle of the trochlear groove [27]. The defect was filled with the ColII-HA-CS-HAP scaffolds containing BMSCs, and the ColII-HA-CS-HAP scaffolds and was not treated. Finally, the lesion was closed using resorbable sutures. Then, all of the rabbits were housed in individual cages and allowed to move freely [28]. The knee joints were removed at 2 months, 4 months and 6 months after the operations. All specimens were then immediately macroscopically examined according to the International Cartilage Repair Society (ICRS) macroscopic cartilage repair assessment [27, 29].

### Histology analysis and immunohistochemistry

The cartilage of the rabbits was fixed with paraformaldehyde overnight (4%) for 72 h, washed was water for 24 h, decalcified in 10% ethylenediaminetetraacetic acid solution, dehydrated in a graded ethanol series, and embedded in paraffin. The samples were processed at 6 μm thickness by sagittal joint sections and stained with safranin O fast green (SOFG, Solarbio, Beijing, China) [30], hematoxylin-eosin (Wuhan Servicebio Technology Co., Ltd, China) [26], toluidine blue (Solarbio, Beijing, China), alcian blue (Wuhan Servicebio Technology Co., Ltd, China) [31] and immunohistochemical staining [32] as previously described. All images were evaluated and scored according to the International Cartilage Repair Society (ICRS) visual histological assessment scale [27, 33, 34].

## Results

### Cultivation and identification of BMSCs

The BMSCs were extracted from New Zealand White rabbits, and identified by hematoxylin and eosin (Figure S1), immunofluorescence staining (Figure S2), flow cytometry analysis (Figure S3) and MTT assays (Figure S4), and a small number of spindle-shaped, multifibrillating, fibroblast-like cells were observed after 3 d of primary culture (Fig. 1A). At 9 d of primary culture, the density of BMSCs reached 90%, and the cells were arranged in spindle-shaped, spiral or parallel bundles (Fig. 1B). The cartilage matrix can naturally induce metachromatic staining, such as toluidine blue metachromatic stains [35]. The results showed that the cytoplasmic color was blue and violet, suggesting that the BMSCs had differentiated into chondrocytes with glycosaminoglycans (Fig. 1C). The results of immunohistochemical staining of collagen type II suggested that the BMSCs also differentiated into chondrocytes (Fig. 1D). The pathological section and HE staining results of mice tissues containing the ColII-HA-CS-HAP scaffolds showed that a small

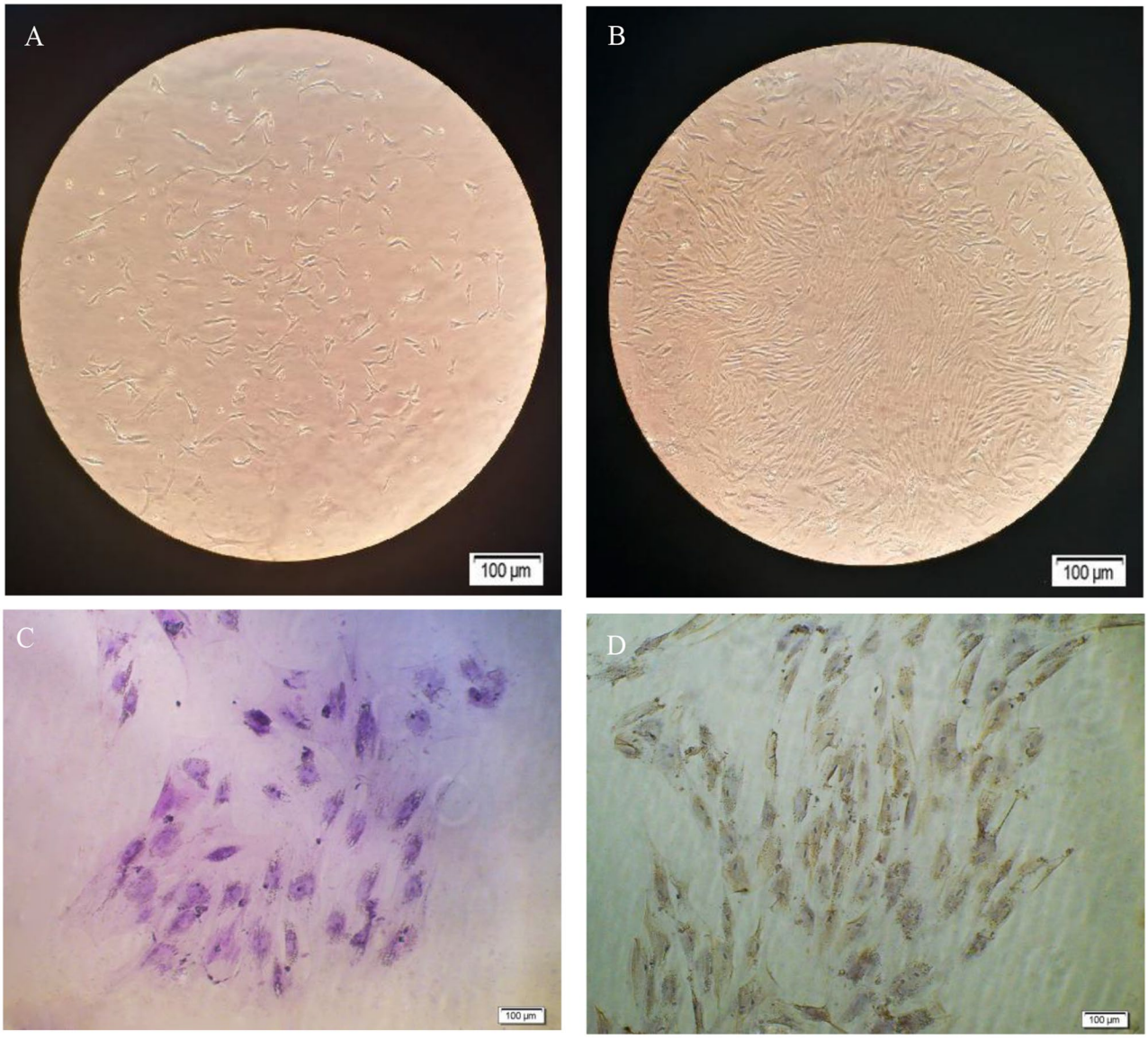


**Fig. 1** Characterization of the BMSCs from New Zealand white rabbit. **A**. The images of the BMSCs were cultured for 3 d. **B**. The images of the BMSCs were cultured for 9 d. **C**. The images of toluidine blue metachromatic staining of the BMSCs. **D**. The images of immunohistochemical staining of Collagen type II. Scale bar: 100 μm

number of lymphocytes accompanied neutrophil infiltration on the fourth day, and then gradually disappeared. No inflammatory cells were observed by microscopy on the tenth day, indicating that the inflammatory response had disappeared (Figure S5).

#### DAPI fluorescent stains

DAPI, as a classical DNA-specific fluorochrome, binds strongly to adenine-thymine-rich sequences of DNA [36], with absorption peaks at 222 nm, 259 nm, and 340 nm, respectively. The fluorescence intensity can easily reflect the DNA content and number of cells when the samples are stained with DAPI [37]. The results of DAPI fluorescence staining showed that the number of BMSCs on the scaffolds increased rapidly. The ColII-HA-CS-HAP scaffolds were conducive to the growth and proliferation of BMSCs, and had good biocompatibility and a reticular shape. In addition, the BMSCs could grow and distribute along the direction of the scaffolds (Fig. 2, Figure S6).

#### Macroscopic examination

The cartilage defects of the blank, control and experimental groups are shown in Fig. 3. When investigated 2 months after implantation, the defects appeared glossy, translucent, and mostly well-integrated in both the control and experimental groups. However, the regenerated cartilage (control group being 45% and experimental group 55%) had a rough and sunken surface. At

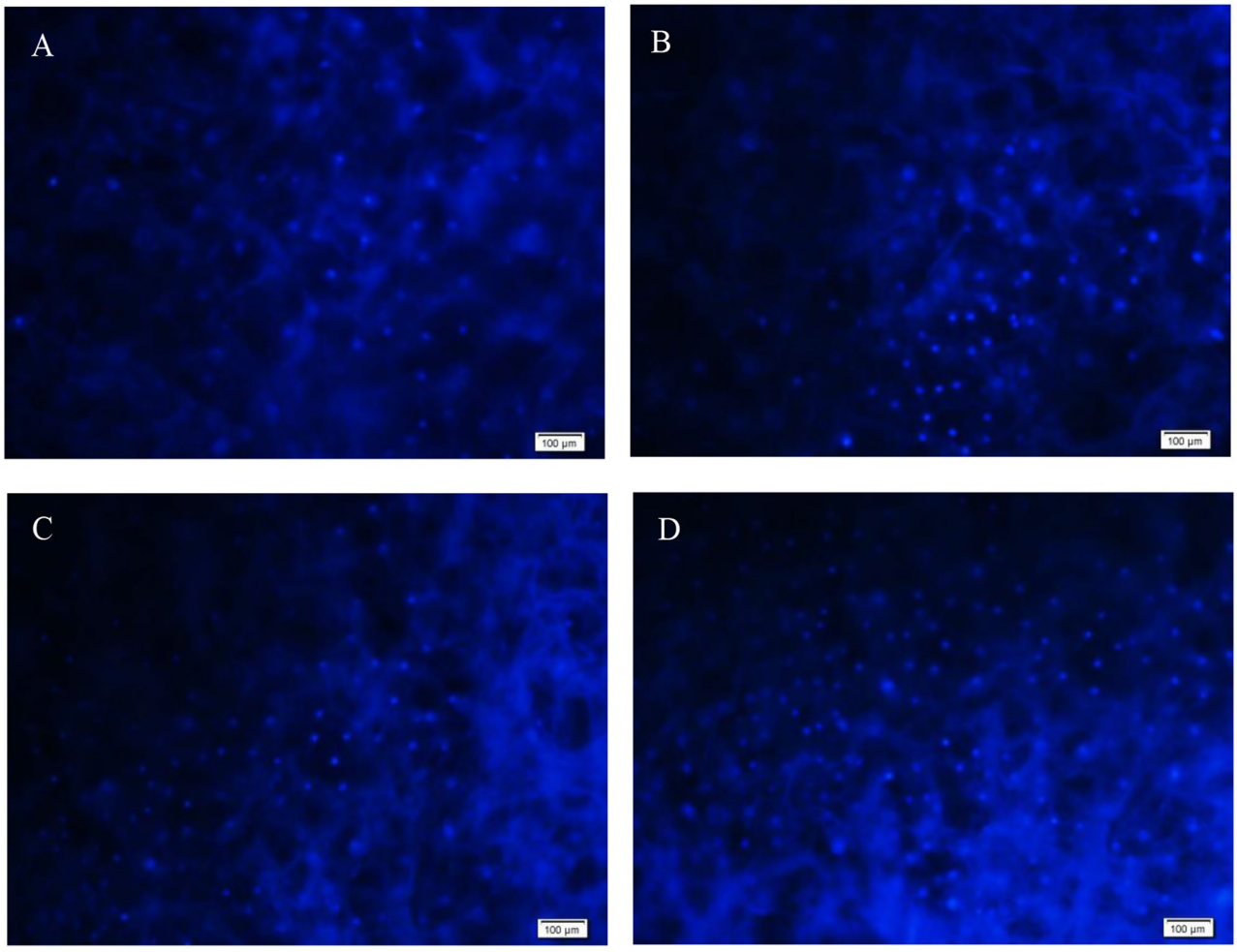


**Fig. 2** The images of DAPI fluorescent stains. **A**. The images of the BMSCs were cultured for 3 d with the ColII-HA-CS-HAP scaffolds. **B**. The images of the BMSCs were cultured for 6 d with the ColII-HA-CS-HAP scaffolds. **C**. The images of the BMSCs were cultured for 9 d with the ColII-HA-CS-HAP scaffolds. **D**. The images of the BMSCs were cultured for 12 d with the ColII-HA-CS-HAP scaffolds. Scale bar: 100 μm

4 months, the regenerated cartilage of the blank group was 25%, while that of the control group was 85% and that of the experimental group was 90%. At 6 months, the regenerated cartilage of the experimental group had reached up to 99%. The interface between the two was not clearly identifiable, while that of the blank group was merely 40% and that of the control group was 93%. The total macroscopic assessment scores (Table S1) were higher in the experimental group than in the control group ($11.40 \pm 0.10$ vs. $10.30 \pm 0.17$; $p < 0.05$), and higher than that of the blank group ($7.33 \pm 0.12$; $p < 0.01$; Fig. 3J, K and L).

Safranin O-fast green (SOFG) staining was used for histological evaluation. The newly formed osteoid was illustrated by the gray-green color, while the cartilage-like tissue was red. The cartilage defect in the control and experimental groups was mended by newly formed osteoid and cartilage-like tissue. In the blank group, only formed osteoid was observed in the defect without cartilage formation apparent at 6 months (Fig. 4).

The hematoxylin-eosin (H&E) stain has stood the test of time as the standard with the capability of highlighting the delicate structures of cells and tissues. The basophilic ribosomes of cartilage cells were dyed blue by hematoxylin, while most eosinophilic cellular organelles and extracellular matrix including collagen fibers were dyed red by eosin [26]. The image results showed that new regenerated tissues, such as osteoid and collagen, were more frequently observed in the region of defects in the experimental group than in the control group after implantation. The soft tissues were predominantly grown into the defects in the blank group (Fig. 5).

The results of SOFG, toluidine blue and alcian blue staining showed poor and slight metachromasia in the blank group, indicating the low proteoglycan content at 6 months post-surgery. The neoformed tissue was dense in the control and experimental groups which represented

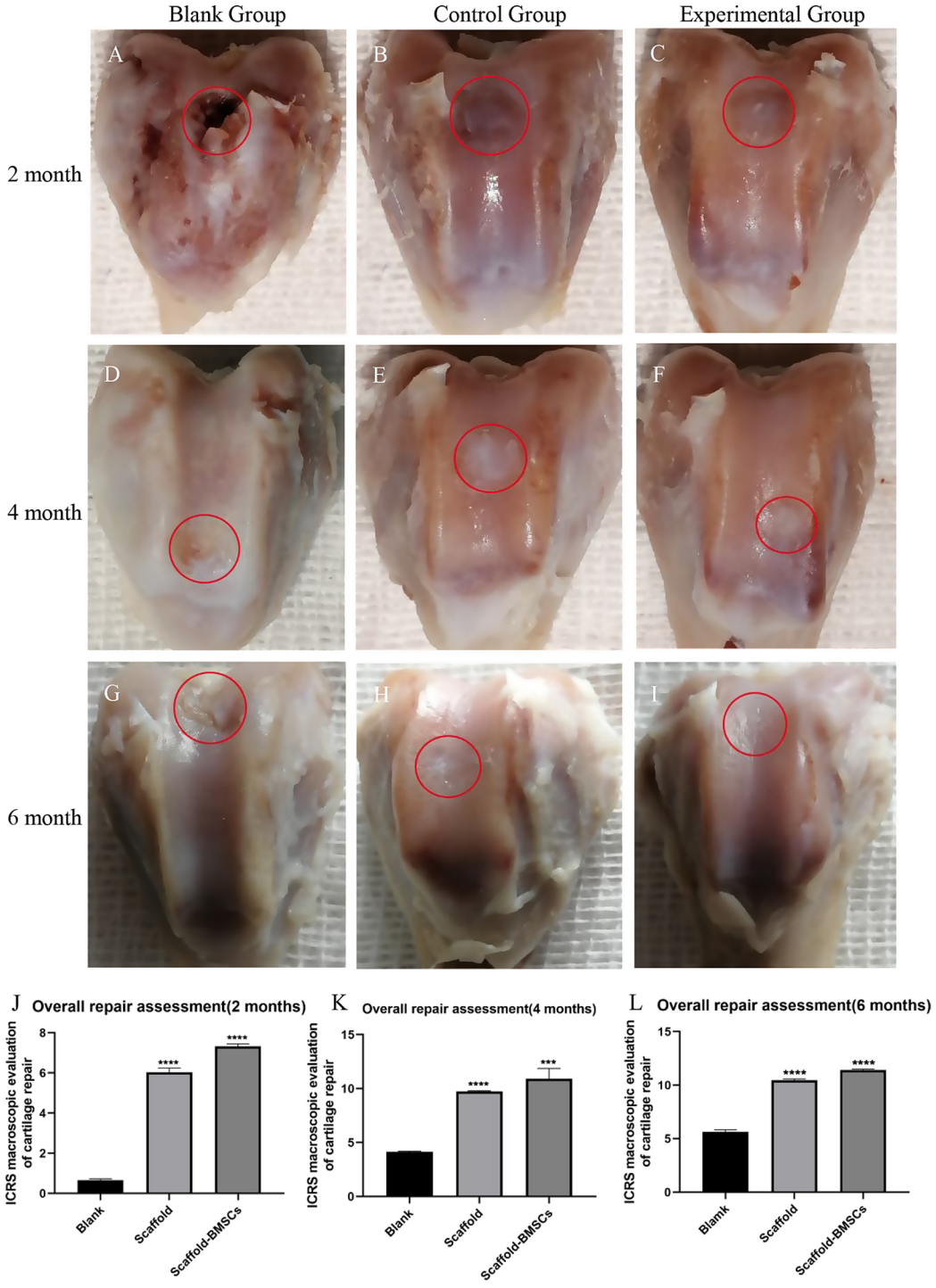


**Fig. 3** Representative photographs of gross appearance of the defect in cartilage (4 mm in diameter) at 2 month (**A**, **B** and **C**), 4 month (**D**, **E** and **F**) and 6 month (**G**, **H** and **I**) after the operations. **A**, **D** and **G** represents cartilage defect model without treatment group (blank group). B, E and H represents treated with the ColII-HA-CS-HAP scaffolds. **C**, **F** and **I** represents treated with the ColII-HA-CS-HAP scaffolds containing the BMSCs. The red circles indicate the original defect margin. **J** (2 month), **K** (4 month) and L (6 month): macroscopic assessment of cartilage repair was assessed by International Cartilage Repair Society (ICRS) macroscopic evaluation scale. Values are the mean ± standard deviation (SD). Asterisks indicate signifificant differences (Student's t-test, $P < 0.01$)

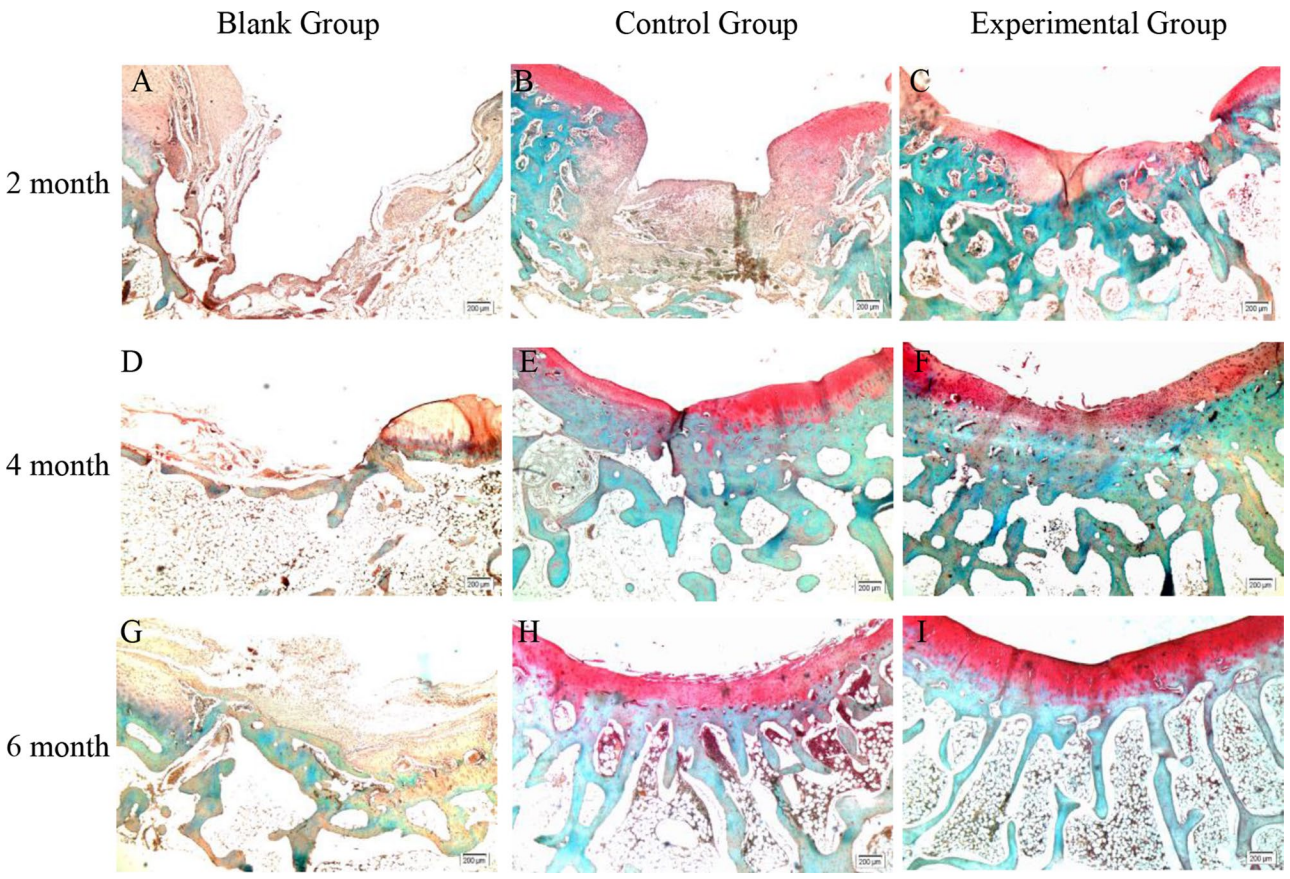


**Fig. 4** The cartilage images of safranin O fast green (SOFG) staining at 2 month (**A**, **B** and **C**), 4 month (**D**, **E** and **F**) and 6 month (**G**, **H** and **I**) after the operations. **A**, **D** and G represents cartilage defect model without treatment group (blank group). **B**, **E** and **H** represents treated with the ColII-HA-CS-HAP scaffolds. **C**, **F** and I represents treated with the ColII-HA-CS-HAP scaffolds containing the BMSCs. Scale bar: 200 μm

higher proteoglycan content. The control group showed lower proteoglycan content than the experimental group (Figs. 4 and 6, Figure S7).

Immunohistochemical staining of the matrix and chondrocytes was dense in the control and experimental groups at 4 and 6 months indicating high expression of ColII (Fig. 7). However, the immunohistochemical intensity staining at 2 months, however, was considerably lower because of the lack of ColII expression in the blank group (Fig. 7A, D and G). ICRS scoring of histological evaluation (Table S2) of cartilage repair revealed a significant difference between the control and experimental groups ($p<0.05$), which was significantly higher than that in the blank group ($p<0.01$) (Fig. 7J-L).

## Discussion

The treatment of knee joint defects represents a challenge in orthopedic surgery [16, 19]. In this study, we evaluated the importance of ColII-HA-CS-HAP scaffolds containing BMSCs in the repair of cartilage defects in a rabbit model.

The ColII-HA-CS-HAP scaffolds, retaining much of the cartilage GAG and ColII, provide a natural microenvironment for BMSC attachment, proliferation, and differentiation into chondrocytes [38]. The results of the DAPI fluorescence stain assay showed that differentiated BMSCs seeded on the ColII-HA-CS-HAP scaffolds underwent rapid growth (Figs. 1 and 2). These results suggest that the ColII-HA-CS-HAP scaffolds have good biocompatibility and nontoxicity.

To examine the regenerative potential of the ColII-HA-CS-HAP scaffolds containing BMSCs, we selected cartilage defects 3 mm in diameter and 4 mm in depth, which are difficult to repair spontaneously (large defect > 3 mm in diameter) [39]. Our findings showed that the regenerated surface of the defect in the ColII-HA-CS-HAP scaffolds containing BMSCs group was very smooth and flat, similar to normal cartilage. The interface of the new cartilage and surrounding normal cartilage was almost indistinguishable at 6 months after surgery (Fig. 3I). At the same time, the defect surfaces in the ColII-HA-CS-HAP scaffold group showed the tissue was thicker and hyaline cartilage-like. The new cartilage was almost identical to the natural cartilage, displaying good integration (Fig. 3H). In contrast, the defect was full of fibrous tissue in the blank group (Fig. 3G).

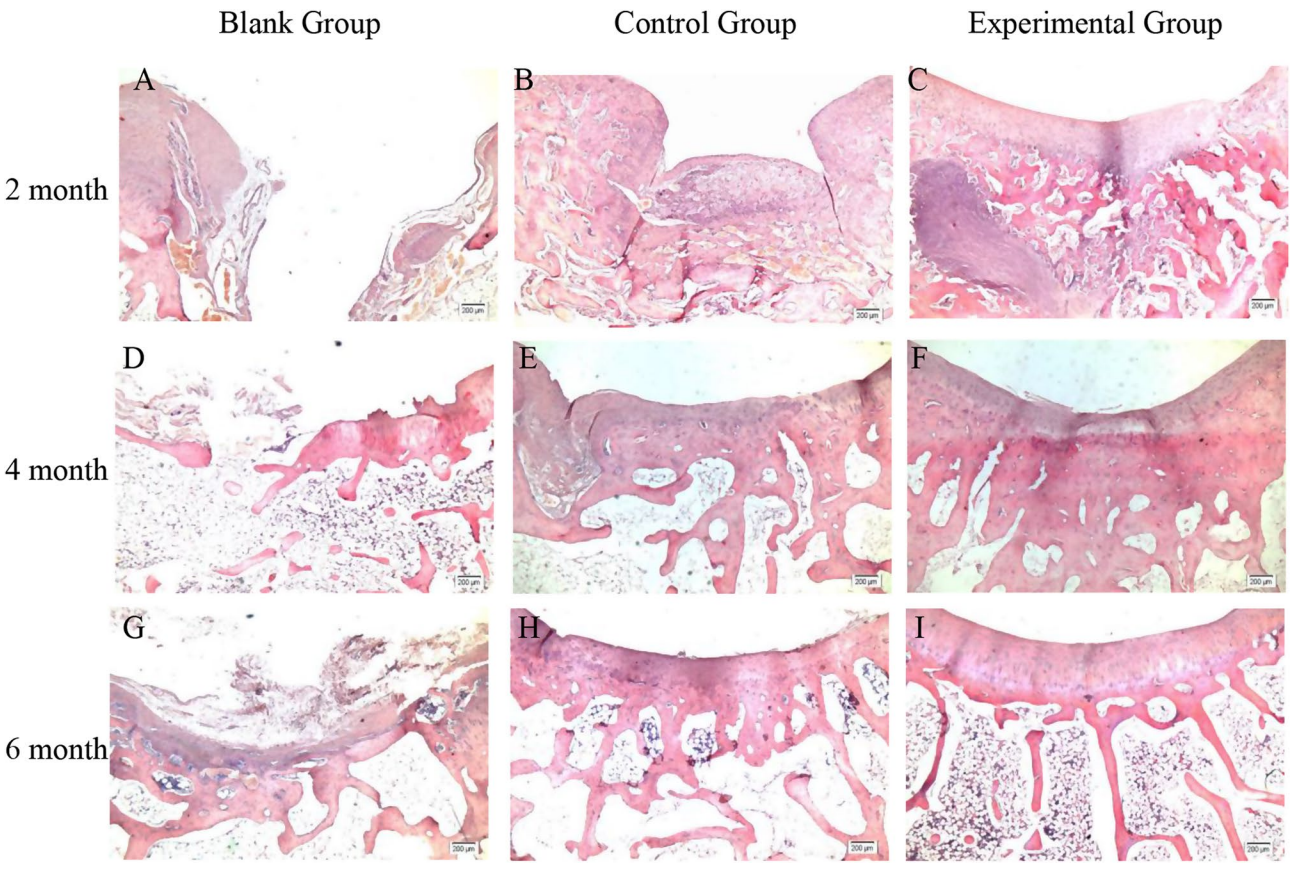


**Fig. 5** The cartilage images of hematoxylin-eosin (HE) staining at 2 month (**A**, **B** and **C**), 4 month (**D**, **E** and **F**) and 6 month (**G**, **H** and **I**) after the operations. **A**, **D** and **G** represents cartilage defect model without treatment group (blank group). **B**, **E** and **H** represents treated with the ColII-HA-CS-HAP scaffolds. **C**, **F** and **I** represents treated with the ColII-HA-CS-HAP scaffolds containing the BMSCs. Scale bar: 200 μm

Cartilage lesions are the most common cause of chronic knee pain [40]. Histological staining and immunohistochemical analysis confirmed that the ColII-HA-CS-HAP scaffolds help chondrocytes differentiated by BMSCs to preserve the hyaline-like chondrogenic cartilage and induce efficient cartilaginous matrix molecules such as proteoglycan secretion and cartilage regeneration (Figs. 4, 5, 6 and 7). These results suggest that the ColII-HA-CS-HAP scaffolds with BMSCs have good biodegradability, and nonimmunogenicity.

In conclusion, our results showed that ColII-HA-CS-HAP scaffolds containing BMSCs with significant physicochemical properties such as biocompatibility, nontoxicity, biodegradability, and nonimmunogenicity could regenerate large osteochondral defects in a rabbit model. The ColII-HA-CS-HAP scaffolds containing BMSCs have a wide range of biomedical applications, such as osteoarthritis surgery, tissue engineering, and drug delivery.

## Conclusions

The ColII-HA-CS-HAP scaffolds with BMSCs were used in the repair of cartilage at first, which is inspired by the biomineralization process, mimiced the composition and structure of bone and low cost, simple operation and green environmental protection tissue engineering cartilage scaffolds. Our research proved that the ColII-HA-CS-HAP scaffolds with differentiated BMSCs can successfully produce a perfect healing response and repair full-thickness cartilage defects in a rabbit model.

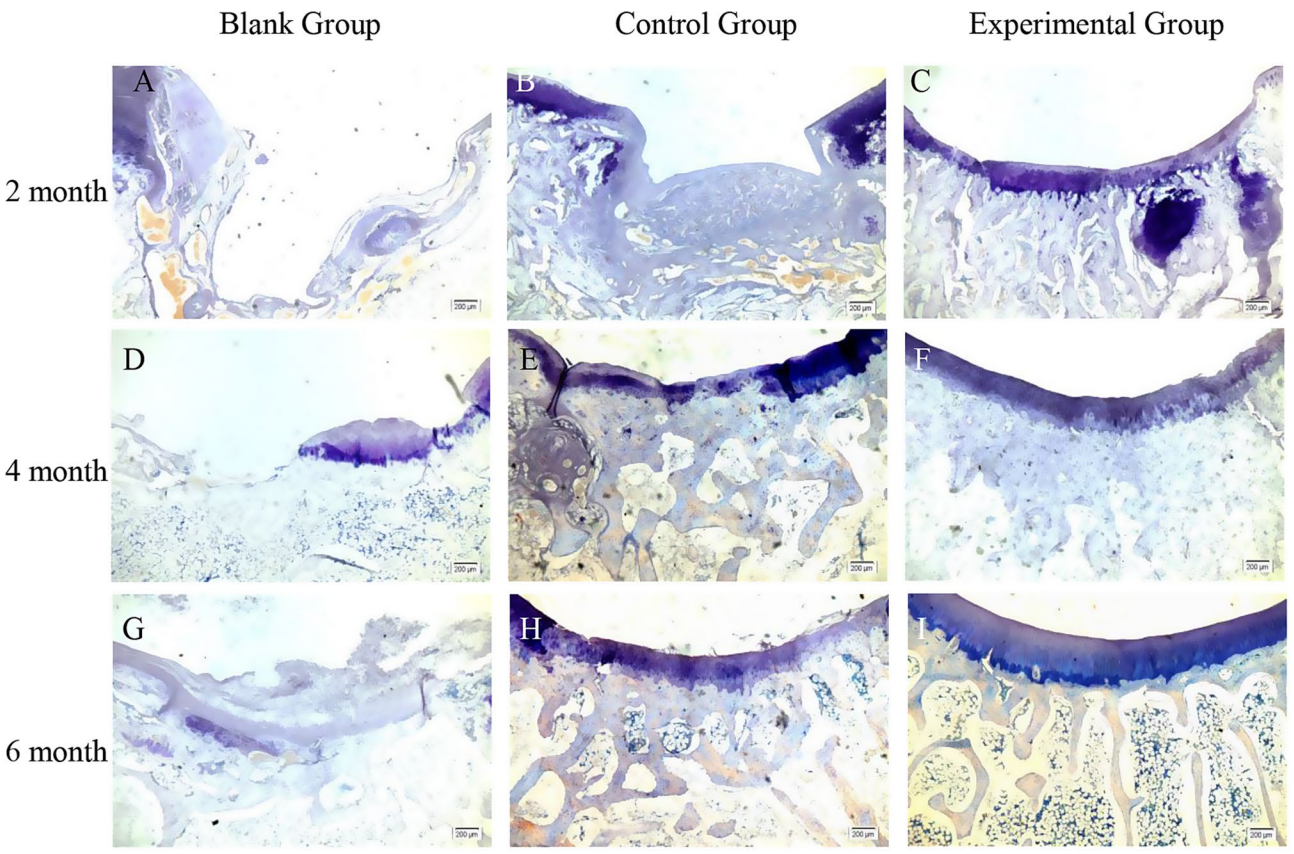


**Fig. 6** The cartilage images of toluidine blue staining at 2 month (**A**, **B** and **C**), 4 month (**D**, **E** and **F**) and 6 month (**G**, **H** and **I**) after the operations. **A**, **D** and **G** represents cartilage defect model without treatment group (blank group). **B**, **E** and **H** represents treated with the ColII-HA-CS-HAP scaffolds. **C**, **F** and **I** represents treated with the ColII-HA-CS-HAP scaffolds containing the BMSCs. Scale bar: 200 μm

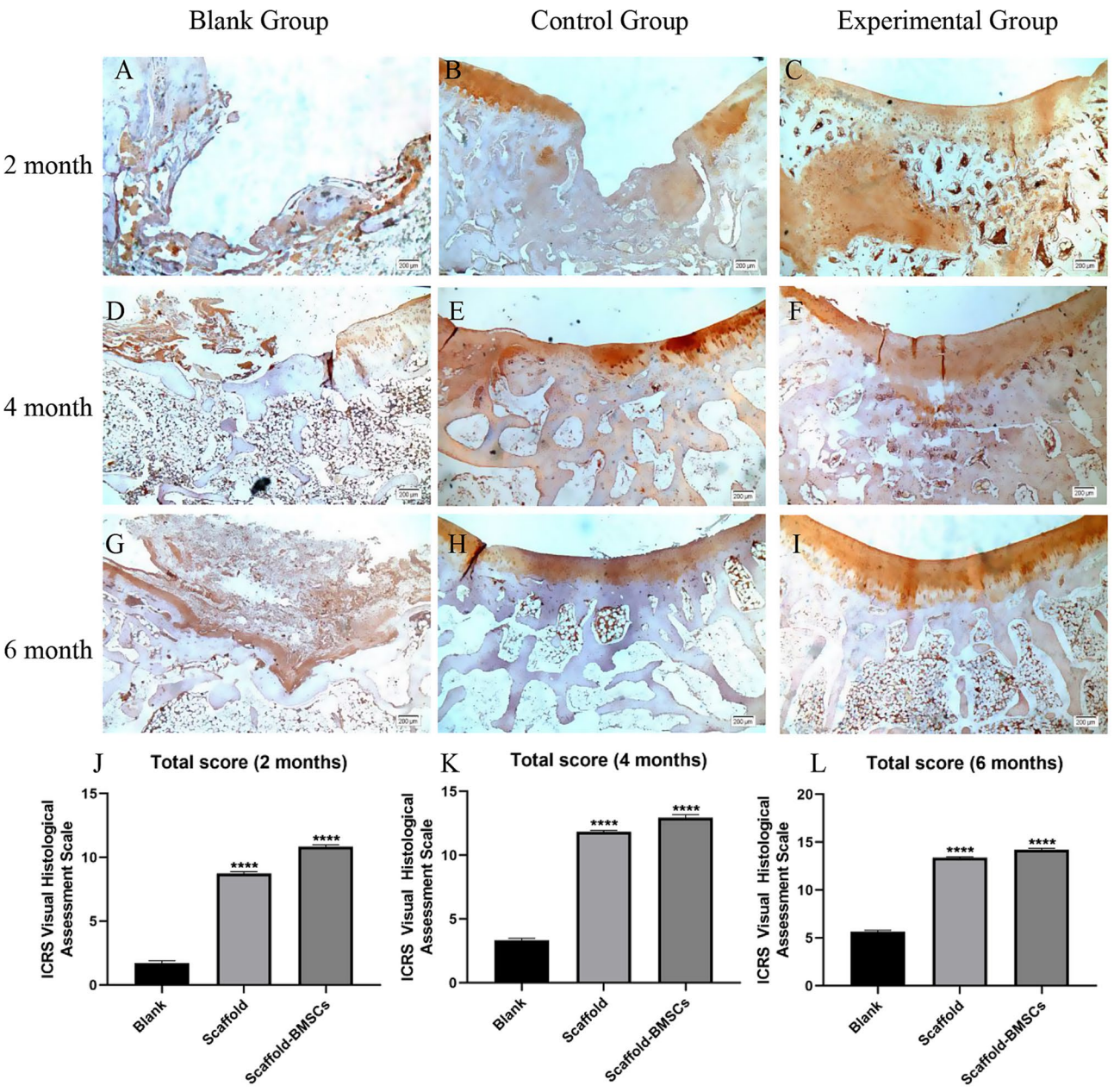


**Fig. 7** The cartilage images of immunohistochemical staining at 2 month (**A**, **B** and **C**), 4 month (**D**, **E** and **F**) and 6 month (**G**, **H** and **I**) after the operations. **A**, **D** and **G** represents cartilage defect model without treatment group (blank group). **B**, **E** and **H** represents treated with the ColII-HA-CS-HAP scaffolds. **C**, **F** and **I** represents treated with the ColII-HA-CS-HAP scaffolds containing the BMSCs. Scale bar: 200 μm. **J** (2 month), **K** (4 month) and **L** (6 month): histochemical assessment of cartilage repair was assessed by International Cartilage Repair Society (ICRS) macroscopic evaluation scale. Values are the mean ± standard deviation (SD). Asterisks indicate signifificant differences (Student's t-test, $P < 0.01$)

## Supplementary Information

The online version contains supplementary material available at https://doi.org/10.1186/s13018-024-05323-5.

Supplementary Material 1

**Acknowledgements**

The authors thank Prof. Wang Fei (The third hospital of hebei medical university, Shijiazhuang, China) for advice on rabbit model and his student Dr. Lu for support with gross appearance of the defect in cartilage.

**Author contributions**

Qiuping Han and Xiaohui Zhou designed and coordinated this study. Qiuping Han, and Xiaoliang He performed the experiments and collected and analyzed the data. Xiaoliang He, Qiuping Han, Yuxin Zhang and Huan Zhang wrote, checked and edited the manuscript. Xiaoliang He , Jun Liu and Xiaohui Zhou provided the funds. All authors have read and approved the final manuscript.

**Funding**

The research was supported by the Natural Science Foundation of Hebei Province (No. H2021208010), Key Project (No.C2020208020), Hebei Province Project for Foreign Experts of Hundred Talents, Project of Advantage and

Characteristic Disciplines in Heilongjiang Province (No. YSTSXK201837) and the Fund of Hebei University of Science and Technology (No. 2021YWF13).

**Data availability**
No datasets were generated or analysed during the current study.

## Declarations

**Competing interests**
The authors declare no competing interests.

Received: 31 October 2024 / Accepted: 28 November 2024
Published online: 03 December 2024

**References**

1. Bian WG, et al. Morphological characteristics of cartilage-bone transitional structures in the human knee joint and CAD design of an osteochondral scaffold. Biomed Eng Online. 2016;15(1):82.
2. Rieppo L, Janssen L, Rahunen K, Lehenkari P, Finnilä MAJ, Saarakkala S. Histochemical quantification of collagen content in articular cartilage. PLoS ONE. 2019;14(11):e0224839.
3. DeAngelis PL. Glycosaminoglycan polysaccharide biosynthesis and production: today and tomorrow. Appl Microbiol Biotechnol. 2012;94(2):295–305.
4. Barat-Houari M, Sarrabay G, Gatinois V, Fabre A, Dumont B, Genevieve D. Isabelle Touitou. Mutation update for COL2A1 gene variants Associated with type II collagenopathies. Hum Mutat. 2016;37(1):7–15.
5. Kobayashi T, Yan H, Kurahashi Y, Ito Y, Maeda H, Tada T, Hongo K, Nakayama J. Role of GalNAc4S-6ST in astrocytic tumor progression. PLoS ONE. 2013;8(1):e54278.
6. Rogers CJ, Clark PM, Tully SE, Abrol R, Garcia KC, Goddard WA 3rd, Hsieh-Wilson LC. Elucidating glycosaminoglycan-protein-protein interactions using carbohydrate microarray and computational approaches. Proc Natl Acad Sci U S A. 2011;108(24):9747–52.
7. Farran A, Montell E, Vergés J, Martel-Pelletier J. Discrepancies in composition and biological effects of different formulations of chondroitin sulfate. Molecules. 2015;20(3):4277–89.
8. Lamparelli EP, Casagranda V, Pressato D, Maffulli N, Della Porta G, Bellini D. Synthesis and characterization of a Novel Composite Scaffold based on hyaluronic acid and equine type I collagen. Pharmaceutics. 2022;14(9):1752.
9. Ciardulli MC, Marino L, Lovecchio J, Giordano E, Forsyth NR, Selleri C, Maffulli N, Porta GD. Tendon and cytokine marker expression by Human Bone Marrow Mesenchymal Stem Cells in a Hyaluronate/Poly-Lactic-co-glycolic acid (PLGA)/Fibrin three-dimensional (3D) Scaffold. Cells. 2020;9(5):1268.
10. Trucillo E, Bisceglia B, Valdrè G, Giordano E, Reverchon E, Maffulli N, Della Porta G. Growth factor sustained delivery from poly-lactic-co-glycolic acid microcarriers and its mass transfer modeling by finite element in a dynamic and static three-dimensional environment bioengineered with stem cells. Biotechnol Bioeng. 2019;116(7):1777–94.
11. Phull AR, Eo SH, Abbas Q, Ahmed M, Kim SJ. Applications of chondrocyte-based Cartilage Engineering: an overview. Biomed Res Int. 2016; 1879837.
12. Migliorini F, Vaishya R, Bell A, Weber CD, Götze C, Maffulli N. Fixation of the membrane during Matrix-Induced Autologous Chondrocyte Implantation in the knee: a systematic review. Life (Basel). 2022;12(11):1718.
13. Kock L, van Donkelaar CC, Ito K. Tissue engineering of functional articular cartilage: the current status. Cell Tissue Res. 2012;347(3):613–27.
14. He A, Liu L, Luo X, Liu Y, Liu Y, Liu F, Wang X, Zhang Z, Zhang W, Liu W, Cao Y, Zhou G. Repair of osteochondral defects with in vitro engineered cartilage based on autologous bone marrow stromal cells in a swine model. Sci Rep. 2017;7:40489.
15. Lamparelli EP, Lovecchio J, Ciardulli MC, Giudice V, Dale TP, Selleri C, Forsyth N, Giordano E, Maffulli N, Della Porta G. Chondrogenic Commitment of Human Bone Marrow Mesenchymal Stem Cells in a perfused collagen hydrogel functionalized with hTGF-β1-Releasing PLGA microcarrier. Pharmaceutics. 2021;13(3):399.
16. Cipollaro L, Ciardulli MC, Della Porta G, Peretti GM, Maffulli N. Biomechanical issues of tissue-engineered constructs for articular cartilage regeneration: in vitro and in vivo approaches. Br Med Bull. 2019;132(1):53–80.
17. Migliorini F, Eschweiler J, Goetze C, Tingart M, Maffulli N. Membrane scaffolds for matrix-induced autologous chondrocyte implantation in the knee: a systematic review. Br Med Bull. 2021;140(1):50–61.
18. Porta GD, Reverchon E, Maffulli N. Biomaterials and supercritical Fluid technologies: which perspectives to fabricate Artificial Extracellular Matrix? Curr Pharm Des. 2017;23(26):3759–71.
19. Migliorini F, Eschweiler J, Schenker H, Baroncini A, Tingart M, Maffulli N. Surgical management of focal chondral defects of the knee: a bayesian network meta-analysis. J Orthop Surg Res. 2021;16(1):543.
20. Nobile C, Maffulli N, Denaro V. Intraoperative application platelet rich fibrin, postoperative injections OF PRP or microfracture only for osteochondral lesions of the knee: a five-year retrospective evaluation. J Biol Regul Homeost Agents. 2016;30(4 Suppl 1):41–9.
21. Liao J, Shi K, Ding Q, Qu Y, Luo F, Qian Z. Recent developments in scaffold-guided cartilage tissue regeneration. J Biomed Nanotechnol. 2014;10:3085–104.
22. Chang CH, Chen CC, Liao CH, Lin FH, Hsu YM, Fang HW. Human acellular cartilage matrix powders as a biological scaffold for cartilage tissue engineering with synovium-derived mesenchymal stem cells. J Biomed Mater Res A. 2013;102(7):2248–57.
23. Tie K, Cai J, Qin J, Xiao H, Shangguan Y, Wang H, Chen L. Nanog/NFATc1/Osterix signaling pathway-mediated promotion of bone formation at the tendon-bone interface after ACL reconstruction with De-BMSCs transplantation. Stem Cell Res Ther. 2021;12(1):576.
24. Meng D, Tanaka H, Kobayashi T, Hatayama H, Zhang X, Ura K, Yunoki S, Takagi Y. The effect of alkaline pretreatment on the biochemical characteristics and fibril-forming abilities of types I and II collagen extracted from bester sturgeon by-products. Int J Biol Macromol. 2019;131:572–80.
25. Akram AN, Zhang C. Extraction of collagen-II with pepsin and ultrasound treatment from chicken sternal cartilage; physicochemical and functional properties. Ultrason Sonochem. 2020;64:105053.
26. Chan JK. The wonderful colors of the hematoxylin-eosin stain in diagnostic surgical pathology. Int J Surg Pathol. 2014;22(1):12–32.
27. Slimi F, Zribi W, Trigui M, Amri R, Gouiaa N, Abid C, Rebai MA, Boudawara T, Jebahi S, Keskes H. The effectiveness of platelet-rich plasma gel on full-thickness cartilage defect repair in a rabbit model. Bone Joint Res. 2021;10(3):192–202.
28. Liu X, Wang L, Ma C, Wang G, Zhang Y, Sun S. Exosomes derived from platelet-rich plasma present a novel potential in alleviating knee osteoarthritis by promoting proliferation and inhibiting apoptosis of chondrocyte via Wnt/β-catenin signaling pathway. J Orthop Surg Res. 2019;14(1):470.
29. van den Borne MP, Raijmakers NJ, Vanlauwe J, Victor J, de Jong SN, Bellemans J, Saris DB. International Cartilage Repair Society. International Cartilage Repair Society (ICRS) and Oswestry macroscopic cartilage evaluation scores validated for use in Autologous Chondrocyte Implantation (ACI) and microfracture. Osteoarthritis Cartilage. 2007;15(12):1397–402.
30. Umiatin U, Hadisoebroto Dilogo I, Sari P, Kusuma Wijaya S. Histological Analysis of Bone Callus in Delayed Union Model Fracture Healing Stimulated with Pulsed Electromagnetic Fields (PEMF). Scientifica (Cairo). 2021; 2021: 4791172.
31. Carton F, Repellin M, Lollo G, Malatesta M. Alcian blue staining to track the intracellular fate of hyaluronic-acid-based nanoparticles at transmission electron microscopy. Eur J Histochem. 2019;63(4):3086.
32. Kamyab-Hesary K, Ghanadan A, Balighi K, Mousavinia SF, Nasimi M. Immunohistochemical staining in the Assessment of Melanoma Tumor Thickness. Pathol Oncol Res. 2020;26(2):885–91.
33. Schmitz N, Laverty S, Kraus VB, Aigner T. Basic methods in histopathology of joint tissues. Osteoarthritis Cartilage. 2010;18(Suppl 3):S113–6.
34. Hoemann C, Kandel R, Roberts S, Saris DB, Creemers L, Mainil-Varlet P, Méthot S, Hollander AP, Buschmann MD. International Cartilage Repair Society (ICRS) recommended guidelines for histological endpoints for cartilage repair studies in animal models and clinical trials. Cartilage. 2011;2(2):153–72.
35. Ribatti D. The staining of mast cells: a historical overview. Int Arch Allergy Immunol. 2018;176(1):55–60.
36. Munyenyembe K, Timmons C, Weiner AKM, Katz LA, Yan Y. DAPI staining and DNA content estimation of nuclei in uncultivable microbial eukaryotes (Arcellinida and Ciliates). Eur J Protistol. 2021;81:125840.
37. Liu K, Lin S, Zhu S, Chen Y, Yin H, Li Z, Chen Z. Hyperspectral microscopy combined with DAPI staining for the identification of hepatic carcinoma cells. Biomed Opt Express. 2020;12(1):173–80.
38. Chang CH, Chen CC, Liao CH, Lin FH, Hsu YM, Fang HW. Human acellular cartilage matrix powders as a biological scaffold for cartilage tissue engineering

with synovium-derived mesenchymal stem cells. J Biomed Mater Res A. 2014;102(7):2248–57.
39. Qi YY, Chen X, Jiang YZ, Cai HX, Wang LL, Song XH, Zou XH, Ouyang HW. Local delivery of autologous platelet in collagen matrix simulated in situ articular cartilage repair. Cell Transpl. 2009;18(10):1161–9.
40. Papalia R, Diaz Balzani L, Torre G, Tirindelli MC, Nobile C, Maffulli N, Denaro V. Intraoperative application platelet rich fibrin, postoperative injections OF PRP or microfracture only for osteochondral lesions of the knee: a five-year retrospective evaluation. J Biol Regul Homeost Agents. 2016;30(4 Suppl 1):41–9.

## Publisher's note